academicJournals

Vol. 8(10), pp. 371-379, 16 March, 2013
DOI: 10.5897/IJPS2013.3851
ISSN 1992-1950 © 2013 Academic Journals
http://www.academicjournals.org/IJPS

International Journal of Physical Sciences

Full Length Research Paper

Temperature dependent current-voltage characteristics of electrodeposited p-ZnO/n-Si heterojunction

Hatice Asil[1], Kübra Çinar[2]*, Emre Gür[2], Cevdet Coşkun[3] and Sebahattin Tüzemen[2]

[1]Faculty of Education, Kilis 7 Aralik University, 79000 Kilis/Turkey
[2]Department of Physics, Faculty of Sciences, Atatürk University, 25240 Erzurum/Turkey.
[3]Department of Physics, Faculty of Arts and Sciences, Giresun University, 28100 Giresun/Turkey.

Accepted 11 March, 2013

p-ZnO thin films were grown by electrochemical deposition (ECD) technique on n-Si substrate in order to form the p-ZnO/n-Si heterojunction. Hall measurement and hot probe techniques were used to determine the conductivity type of the ECD grown ZnO thin film. X-ray diffraction measurements revealed the peaks corresponding to the ZnO crystal directions of (002), (101) and (200) confirmed by the Joint Committee on Powder Diffraction Standards (JCPDS) files, indicating the polycrystalline nature of the films. The electrical characterization of p-ZnO/n-Si heterojunction was carried out in the temperature range of 80-300 K. The ideality factor and barrier height of the structure exhibited a variation between 2.49 to 5.36 and between 0.574 and 0.173 eV for this temperature ranges, respectively. The variation with temperature observed on the electrical parameters of the p-ZnO/n-Si heterojunction was explained by the introduction of a spatial distribution of barrier heights due to barrier height in homogeneities that prevail at the p-ZnO/n-Si heterojunction interface.

Key words: ZnO thin films, p-n heterojunction, electrodeposition.

INTRODUCTION

ZnO is a member of II-VI compound semiconductor family which has a wide and direct band-gap of about 3.4 eV. Its physical properties such as high transparency, large excitonic binding energy of 60 meV, wurtzite crystal structure (almost the same lattice parameters with GaN), resistance to high energy radiation and temperature makes it very attractive for both optical and electrical devices. Many ZnO based devices have been already reported such as lasers (LDs) (Buzás and Geretovszy, 2007) and light emitting diodes (LEDs) (Guo et al., 2008) working in ultraviolet region and thin film transistors (TFTs) (Fortunato et al., 2005; Kim et al., 2009) for solid-state electronics. Also, it can be easily grown with any growth technique since Zn is one of the most easily oxidized elements. Variety of growth methods have been used to grow ZnO thin films so far, such as chemical vapor deposition (Sen Chien et al., 2010), ionized cluster-beam deposition (Whangbo et al., 2000), pulsed laser deposition (Zhu et al., 2010), DC sputtering (Ye et al., 2003) and magnetron sputtering (Kim et al., 2003), metal organic chemical vapour deposition (MOCVD) (Mohanta et al., 2008), sol-gel method (Li et al., 2010), chemical spray pyrolysis (Krunks et al., 2009) and electrochemicaldeposition (ECD) (Sharma et al., 2010; Cembrero and Busquets-Mataix, 2009; Dalchiele et al., 2001; Inguanta et al., 2013; Mouet et al., 2010). ECD growth technique has a number of advantages that makes it ideal for some specific applications, which are being low cost, allowing growth of thin films with large area at low temperature, controllable thickness and deposition rate which is relatively higher than other techniques (Izaki and Omi, 1997). The technique is also

*Corresponding author. E-mail: kubrac25@gmail.com. Tel: +90 442 231 4383. Fax: +90 442 236 0948.

less hazardous and more environmentally friendly (Izaki and Katayama, 2000). One of the most important challenges of ZnO based technologies which is preventing the progress in device arena is difficulty in obtaining p-type conductivity. Although first p-type conductivity in ZnO reported in 1997, it has still been difficult to deposit p-type ZnO with high homogeneity, quality and purity for optoelectronic device applications. However, a lot of different doping elements have been reported as a source of p-type conductivity such as N, Li, Mg, K, Cu, Na, As, P, Sb, Ag, etc. (Liu et al., 2008; Xiao et al., 2006; Fang and Kang, 2010; Jun and Yintang, 2008; McCluskey and Jokela, 2009; Janotti and Van de Wall, 2009; Kim et al., 2009; Lin et al., 2008; Fan et al., 2007; Doggett et al., 2007; Pan et al., 2007; Kim et al., 2009). The most promising, reliable and preferable one is doping with only N and co-doping N with group III elements (Tüzemen and Gür, 2007).

Zn_3N_2 powder was used to obtain p-type ZnO in the present study, which was shown previously that annealing Zn_3N_2 powder in oxygen media helps to obtain p-ZnO (Zou et al., 2009; Kaminska et al., 2005). Also, Wang et al. (2003) and Erie et al. (2008) reported that ZnO thin films doped with Zn_3N_2 deposited by DC magnetron sputtering and pulsed laser deposition techniques are resulted in p-type conductivity.

In this study, we performed the p-type growth of ZnO thin film on n-type Si substrate using ECD technique in order to investigate the electrical characteristics of p-ZnO/n-Si heterojunction. The electrical parameters of p-ZnO/n-Si heterojunction were determined with current-voltage (I-V) measurements in the temperature range of 80-300 K.

EXPERIMENTAL

Before forming the p-ZnO/n-Si heterojunction, n-Si (100) substrate were cleaned using the root cause analysis (RCA) procedure (waited in boiling $NH_3+H_2O_2+6H_2O$ for 10 min and then, $HCl+H_2O_2+6H_2O_2$ at 60°C for 10 min) as reported in literature (Aydoğan et al., 2009). Then, Zn_3N_2 powder was spread out on n-Si wafer and annealed at 450°C for one hour to obtain a homogeneous film on the Si substrate. The electrochemical growth process was carried out by using an electrochemical cell having three electrodes which are counter (Zn), reference (Ag/AgCl) and working electrodes (n-Si). The growth process was controlled by a Gamry Reference 600 Potentiostat-Galvanostat/ZRA (Zero Resistance Ammeter). For p-ZnO growth, we prepared a solution of 0.05 M $Zn(ClO_4)_2$ and 0.1 M $Li(ClO_4)$ in dimethyl sulfoxide [DMSO-$(CH_3)_2SO$] as a solution. The ECD growth was carried out under the cathodic potential of -1 V and lasted one hour at solution temperature of 130°C. After deposition, sample was cleaned with de-ionized water.

Indium is used as an ohmic contact material on both sides of the structure which can be seen in Figure 1. The conductivity type of the ZnO thin films was determined using the Hall and resistivity measurements and hot probe technique. The Hall measurements were performed by a home-made Hall kit using a Varian 2901 regulated magnet power supply. The carrier concentration, resistivity and mobility parameters were calculated from Hall measurements. The I-V characteristics of p-ZnO/n-Si heterojunction were obtained by using a Keithley 487 picoammeter equipped with a closed-cycle helium cryostat. The samples were also characterized by X-ray diffraction (XRD) technique structurally using Rigaku D/Max-IIIC diffractometer, with Cu Kα radiation of 1.54 Å, within the 2θ angle ranging from 20-80°.

RESULTS AND DISCUSSION

Michael Faraday reported that the thickness of the film can be calculated with the help Faraday's laws of electrolysis focused on the electrochemical researches in 1834 as follows:

$$F=mQ/(\rho.n.A.t) \quad (1)$$

$$d=mQ/(nFA\rho) \quad (2)$$

where are d is the thin film tickness, A; the surface area, F; Faraday's number (96485 C/mol), n; the charge number (2 for ZnO), Q; the charge passed, ρ; density (5.6 g/cm^3), m; the molecular weight (81.4 g/mol). We have calculated about 1.5 µm to the thickness of the thin film with the help of this formula.

Figure 2 shows XRD pattern of ECD grown p-type ZnO thin film on n-Si substrate. The ZnO crystal planes of (002), (101) and (200) confirmed by the Joint Committee on Powder Diffraction Standards (JCPDS) files (36-1451 and 65-0682) can be clearly seen which indicates the polycrystalline structure of the grown thin films. The full width at half maximum (FWHM) values of the peaks corresponding to the (002), (101) and (200) planes are 0.094, 0.312 and 0.086, respectively. In addition, grain sizes of the (002) and (101) peaks were calculated as 88.54, 26.7 and 98.8 nm, respectively.

The p-type conductivity of the grown ZnO thin film was confirmed by both hot probe and Hall measurements with the Van der Pauw configuration. The carrier concentration and Hall voltage of p-ZnO thin film were determined as 3×10^{15} cm^{-3} and 0.986 mV using Hall measurement technique, respectively.

Figure 3 demonstrates both forward and reverse bias log (I-V) plot of p-ZnO/n-Si hetero junction. The current flow through a p-n junction can be defined by thermionic emission (TE) theory as follows (Rhoderick and Williams, 1998):

$$I = I_0 \exp\left(\frac{qV}{nkT}\right)\left[1-\exp\left(-\frac{qV}{kT}\right)\right] \quad (3)$$

where q is the electronic charge, k Boltzmann constant, T temperature, V the applied voltage, n ideality factor which is given by:

$$n = \frac{q}{kT}\left(\frac{dV}{d(\ln I)}\right) \quad (4)$$

I_0 is the reverse saturation current which is obtained

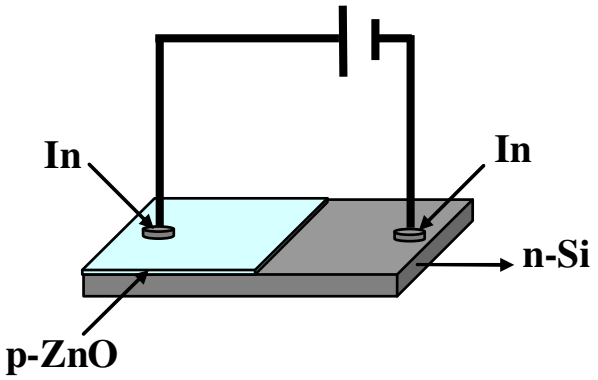

Figure 1. The schematic diagram of the p-ZnO/n-Si heterojunction

from the straight line intercept of $\ln I$ at $V = 0$ in Equation (3) and is given:

$$I_0 = A^* A T^2 \exp\left(-\frac{q\Phi_{b0}}{kT}\right) \quad (5)$$

where A^* is the effective Richardson constant, A the diode area and the zero-bias barrier height.

The experimental values of n and Φ_{b0} can be determined from intercepts and slopes of the forward bias I-V plot at each temperature (Figure 3) using Equations (4) and (5), respectively. n and Φ_{b0} values of the p-ZnO/n-Si heterojunction exhibit a variation between 2.49 and 0.574 eV at 300 K and 5.36 and 0.173 eV at 80 K, respectively. There may be a mixture of different metallic phases with different barrier heights (BHs) at heterojunction interface due to incomplete interfacial reaction. Image force-lower, generation-recombination, interface states and TFE are the mechanisms caused the large values of the ideality factor. The absolute value of ideality factor can be determined by the help of these calculated mechanisms. Also, the contamination at a interface is often present at the interfaces of junction prepared by the routine processing methods used in the semiconductor electronics industries. These contaminants may act directly to introduce inhomogeneity or they may simply promote inhomogeneity, through the generation of defects, additional interfacial chemical phases and etc. Even if the absence of chemical contaminants, BH inhomogeneity may be present. Thus, interface roughness may contribute to the presence of BH inhomogeneity due to effectively increasing or decreasing the low-BH patches. Finally, there are numerous structural defects, grain boundaries, dislocations, stacking faults, at interfaces, and these may contribute to BH inhomogeneity (Sullivan et al., 1991; Soylu and Yakuphanoglu, 2010; Tung, 1992).

Figure 4 shows the variation of ideality factor and barrier height with temperature. As can be seen in Figure 4, the values of n are indicated by the open triangles (experimental) and the closed triangles show estimated value of ideality factor using Equation (12) with coefficients ρ_2 and ρ_3. The values of Φ_{b0} by the open squares (experimental) and the closed squares represent estimated values of Φ_{b0} using Equation (11) with σ_{s0}. While Φ_{b0} increases with increasing temperature, n decreases. This behavior may be explained by current flow through the patches of lower barrier height and larger ideality factor and has been successfully explained on the basis of TE mechanism which takes into consideration spatial distribution of the barrier heights due to the inhomogeneities prevailing at the p-n junction interface. Since current transport across the interface is a temperature activated process, electrons at low temperatures are able to surmount the lower barriers and therefore, the current transport will be dominated by current flow through the patches of lower barrier height (BH) and a larger ideality factor. As the temperature increases, more and more electrons have sufficient energy to surmount the higher barrier (Sullivan et al., 1991; Tung, 1992; Biber et al., 2002; Karataş et al., 2003; Güllü et al., 2007).

A conventional activation $\ln(I_0/T^2)$ energy $1/kT$ versus $1/nkT$ or plot is shown in Figure 5. $\ln(I_0/T^2)$ versus $1/kT$ plot is found to be non-linear in the measurement temperature range. The non-linearity of $\ln(I_0/T^2)$ versus $1/kT$ plot is caused by the temperature dependence of the barrier height and ideality factor. According to Equation (5), one obtains:

$$\ln\left(\frac{I_0}{T^2}\right) = \ln(AA^*) - \frac{q\Phi_{b0}}{kT} \quad (6)$$

According to Equation (6), the plot yields a straight line with a slope given by a barrier height at 0 K, $\Phi_{b0}(T=0)$ and intercept is the Richardson constant (A*). This straight line yields activation energy of 0.257 eV, as shown in Figure 5. The deviation in the Richardson constant may be due to the spatial distribution of inhomogeneous barrier heights and potential fluctuations at the interface that consist of low and high barrier areas (Tung, 1992; Karataş et al., 2003; Güllü et al., 2007).

The Richardson constant obtained from $\ln(I_0/T^2)$ versus $1/kT$ plot was determined as 1.53 × 10^{-7} A/cm^{2}K^2. This value obtained from the temperature dependence of the $I-V$ characteristics may also be affected by lateral in homogeneities of the barrier heights. This discrepancy can be explained by supposing that the distribution of the barrier heights is a Gaussian distribution of barrier heights with a mean value $\overline{\Phi}_b$ and standard deviation σ_s, in the form of:

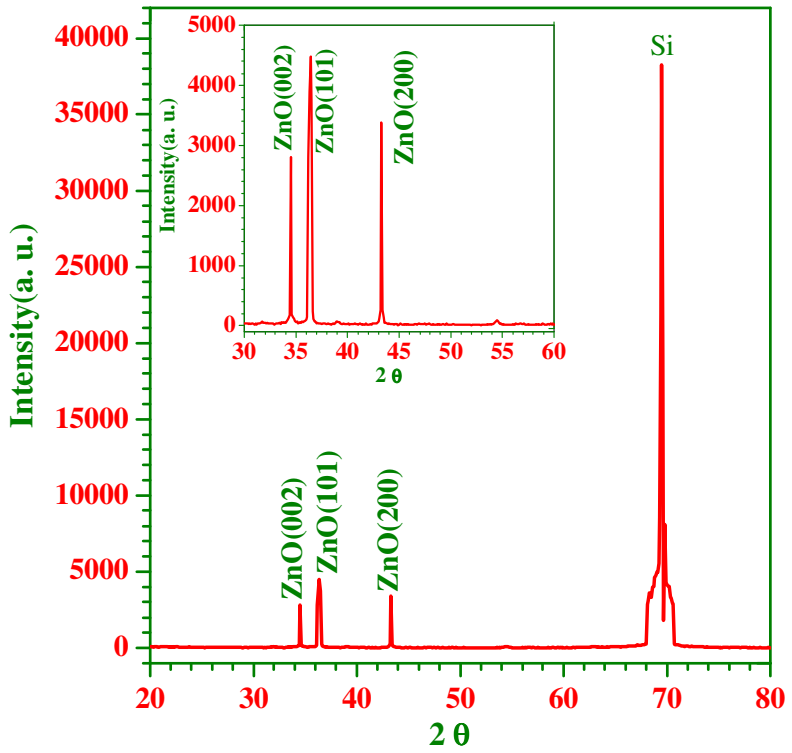

Figure 2. XRD measurement result of the p-type ZnO thin film deposited on n-Si substrate.

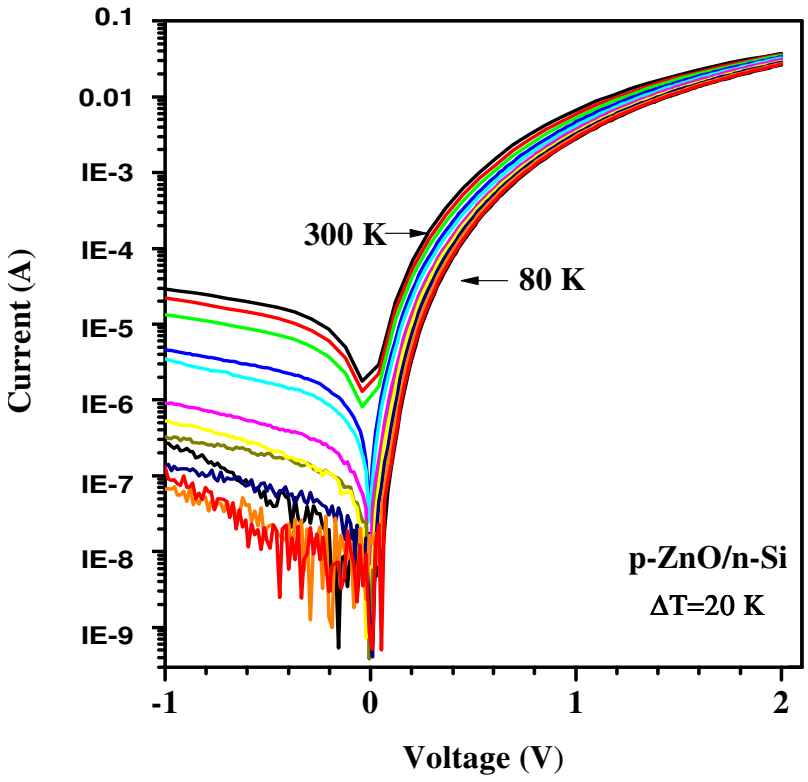

Figure 3. The current-voltage characteristics of the p-ZnO/n-Si heterojunction at temperature between 80-300K.

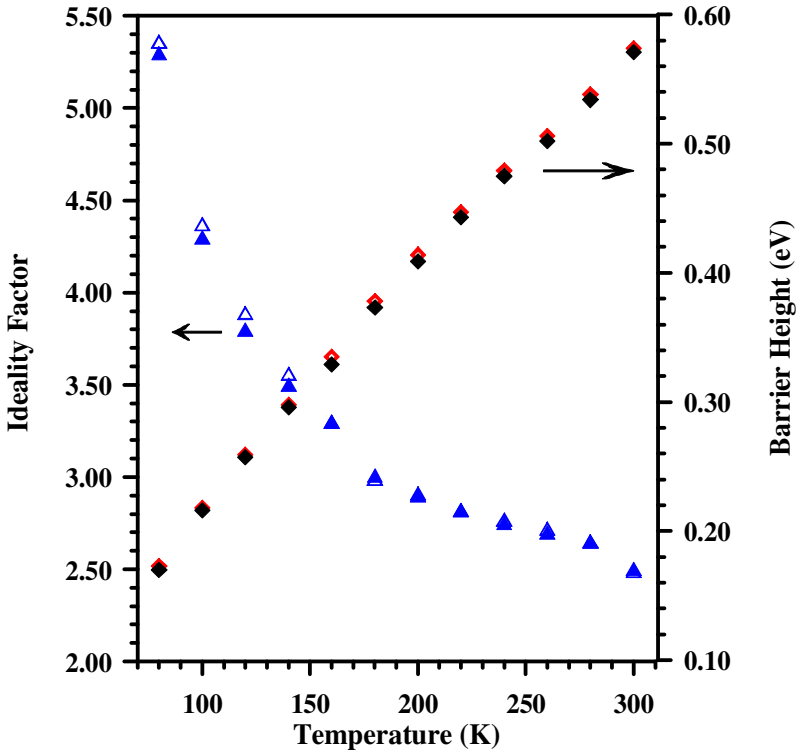

Figure 4. The ideality and barrier height versus temperature plots for p-ZnO/n-Si heterojunction.

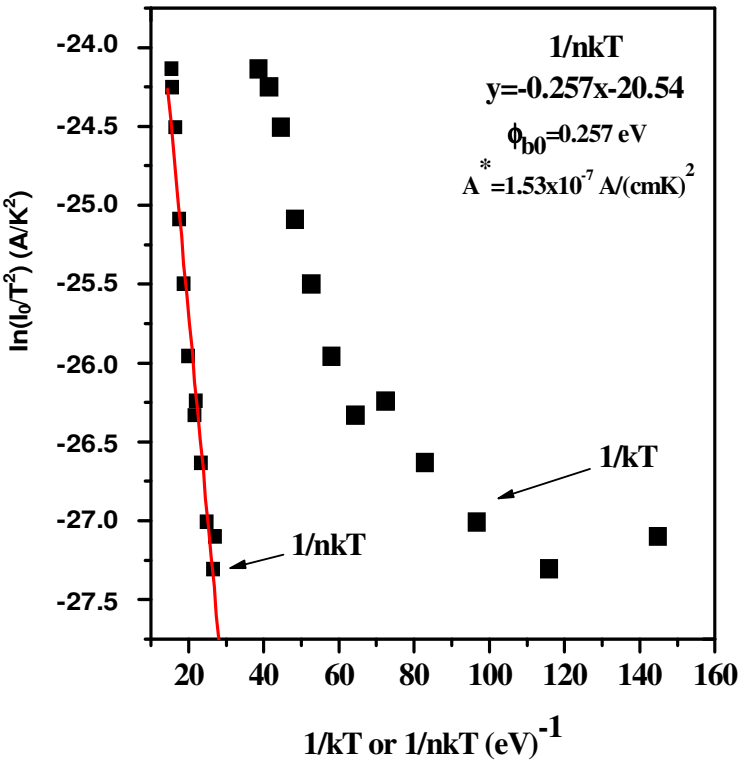

Figure 5. The $\ln\left(I_0/T^2\right)-1/kT$ or $1/nkT$ plot for heterojunction.

$$P(\Phi_b) = \frac{1}{\sigma_s\sqrt{2\pi}} \exp\left(-\frac{\left(\Phi_b - \bar{\Phi}_b\right)^2}{2\sigma_s^2}\right) \quad (7)$$

where $1/\sigma_s\sqrt{2\pi}$ is the normalization constant of the Gaussian barrier height distribution. The total current under the forward bias of V can be expressed as:

$$I(V) = \int_{-\infty}^{+\infty} I(\Phi_b, V) P(\Phi_b) d\Phi \quad (8)$$

where $1/\sigma_s\sqrt{2\pi}$ is the current at the bias for a barrier height based on the ideal thermionic emission-diffusion theory and $P(\Phi_b)$ is the normalized distribution function giving the probability of accuracy for barrier height. Upon integration,

$$I(V) = A * T^2 \exp\left[-\frac{q}{kT}\left(\bar{\Phi}_b - \frac{q\sigma_s^2}{2kT}\right)\right] \exp\left(\frac{qV}{n_{ap}kT}\right) x\left[1 - \exp\left(\frac{qV}{kT}\right)\right] \quad (9)$$

with

$$I_0 = AA * T^2 \exp\left(-\frac{q\Phi_{ap}}{kT}\right), \quad (10)$$

where Φ_{ap} and n_{ap} are the apparent barrier height and apparent ideality factor , respectively, and are given by:

$$\Phi_{ap} = \bar{\Phi}_{b0} - \frac{q\sigma_{s0}^2}{2kT} \quad (11)$$

$$\left(\frac{1}{n_{ap}} - 1\right) = \rho_2 + \frac{q\rho_3}{2kT} \quad (12)$$

In Equation (12), ρ_2 and ρ_3 values are the coefficients of voltage deformation of the barrier distribution. That is, the voltage dependencies of the mean barrier height and the barrier distribution width are given by coefficients and ρ_2 and ρ_3, respectively. Then, σ_{so} is the zero bias standard deviation of barrier height distribution. The standard deviation is a measure of the barrier homogenity. Song et al. (1986) and Werner and Güttler (1991) were used in the above expression for the apparent barrier homogeneity construction. If standard deviation is small it can be neglected. The temperature dependence of the ideality factor can be understood on the basis of Equation (12). The plot of n_{ap} versus $1/2kT$ should give a straight line that gives voltage coefficients ρ_2 and ρ_3 from intercept and slope respectively, as shown in Figure 6. The ρ_2 values from the slope of $(n^{-1}-1)$-$(1/2kT)$ plot were obtained as -0.515 at a temperature range between 300-160K and determined as -0.586 for 160-80K, respectively. Also, the ρ_3 values from the same plot were determined as -0.0049 for 300-160 K range and then measured as -0.0031 at for the range of 160-80K. $\bar{\Phi}_{bo}$ and σ_{s0} values were calculated from the slope of barrier height vs. (1/2kT) plot (Figure 7). $\bar{\Phi}_{bo}$ and σ_{s0} were measured as 0.818 eV and 117 mV at the range 300-160K while they were determined as 0.481 eV and 54 mV between 160-80K, respectively.

The continuous solid line in Figure 7 represents data estimated with these parameters using Equation (11). Combining the Equations (10) and (11), we get:

$$\ln\left(\frac{I_0}{T^2}\right) - \left(\frac{q^2\sigma_0^2}{2k^2T^2}\right) = \ln(AA*) - \frac{q\bar{\Phi}_{b0}}{kT} \quad (13)$$

According to Equation 13, a modified $\ln(I_0/T^2) - (q^2\sigma_0^2/2k^2T^2)$ versus $1/T$ plot should give a straight line with the slope directly performed by the mean and the intercept (=lnAA*) at the ordinate, determining A* for a given diode area A. Figure 8 shows $\ln(I_0/T^2) - (q^2\sigma_0^2/2k^2T^2)$ versus $1/T$ plot. The $\ln(I_0/T^2) - (q^2\sigma_0^2/2k^2T^2)$ versus $1/T$ plot yielded $\bar{\Phi}_{bo}$ of 0.794 eV in the range of 300-160K and 0.329 eV in the range of 160-80K, respectively. These values are convenient with what it is obtained from the mean BHs as shown in Figure 7. Richardson constant is obtained as 0.011 A/cm^{2}K^2 in the range of 160-80 K and 6.235 A/cm^{2}K^2 for 300-160K from the modified activation energy plot, respectively.

Conclusion

p-ZnO thin films were deposited by ECD technique on n-Si substrate to obtain p-ZnO/n-Si heterojunction. The I-V characteristics of the electrochemically fabricated p-ZnO/n-Si heterojunction were measured at a temperature range of 80-300 K. It is observed that the ideality factor of p-ZnO/n-Si heterojunction increases while the barrier height decreases within this temperature range. The I-V characteristics of this structure have been interpreted on the basis of TE mechanism with Gaussian distribution of the barrier heights. Richardson constant is calculated between 0.011-6.235 A/cm^{2}K^2 for the temperature range of 300-80 K from $\ln(I_0/T^2) - q^2\sigma^2_{s0}/2k^2T^2 - 1/kT$ plot.

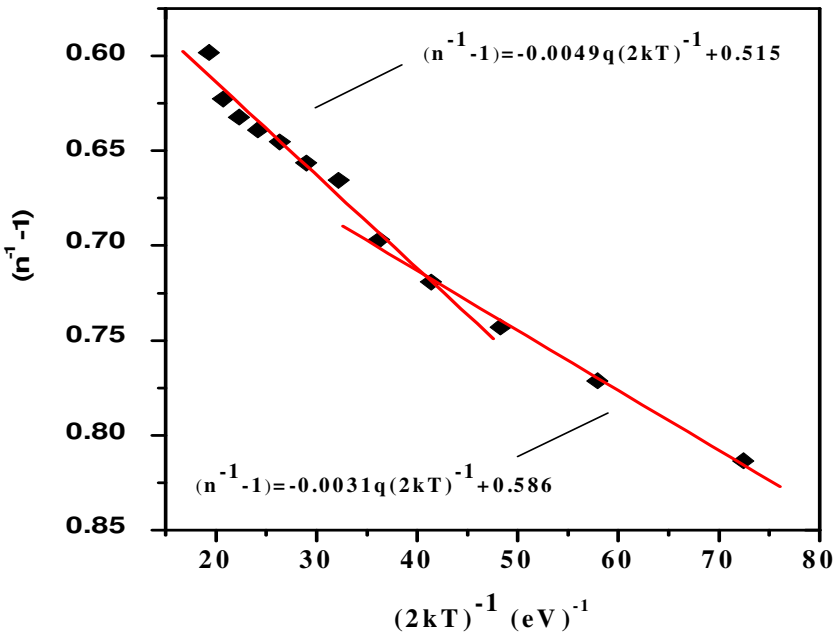

Figure 6. $(n^{-1}-1)$ versus $(1/2kT)$ plot of the p-ZnO/n-Si heterojunction. The continuous curves show estimated values of ideality factor using Eq. (10) for Gaussian distributions of barrier heights with $\rho_2 = -0.515$, $\rho_3 = -0.0049$ V in 300-160 K and $\rho_2 = -0.586$, $\rho_3 = -0.0031$ V in 160-80 K.).

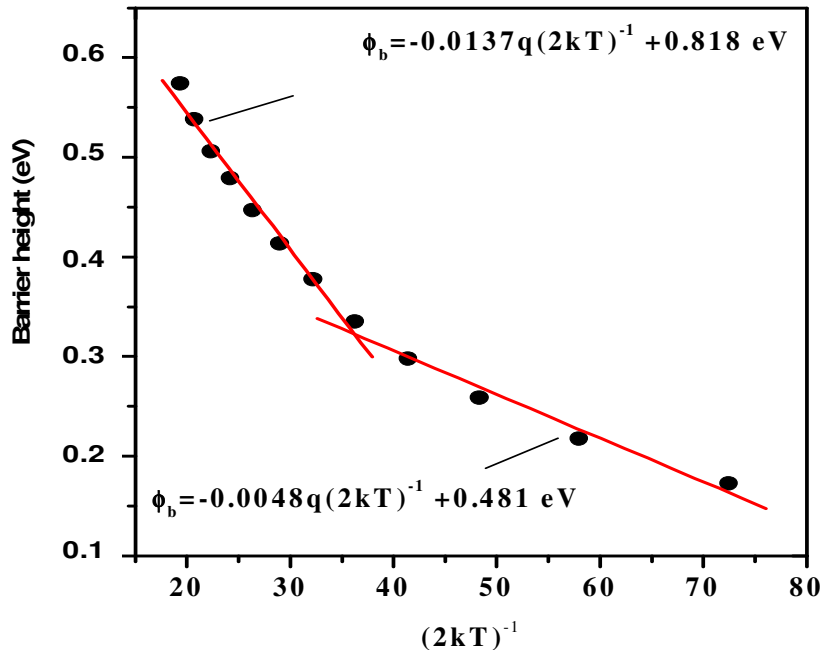

Figure 7. The barrier height-1/(2kT) curve of the p-ZnO/n-Si hetrojunction. The continuous curve related to the filled circles represents estimated values of Φ_{ap} using Equation (9) for Gaussian distributions of barrier heights with $\bar{\Phi}_{b0} = 0.818$ eV and $\sigma_{s0} = 117$ mV in 300-160 K and $\bar{\Phi}_{b0} = 0.481$ eV and $\sigma_{s0} = 54$ mV in 160-80K.

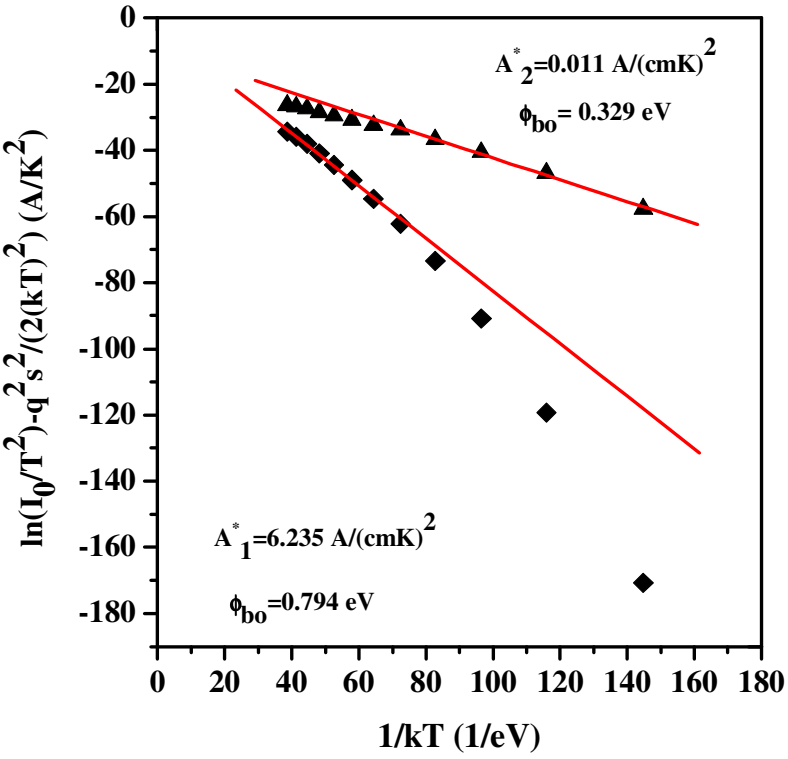

Figure 8. The $\ln(I_0/T^2)-q^2\sigma^2_{s0}/2k^2T^2-1/kT$ plot for the heterojunction according to Gaussian distributions of the barrier heights. The filled triangels represent the plot calculated for $\sigma_{s0}=117$ mV in 300-160 K and the filled squares represent the plot calculated for $\sigma_{s0}=54$ mV in 160-80 K.

ACKNOWLEDGEMENTS

We would like to thank Dr. Şakir Aydoğan for his help in the preparation of the paper. This work was carried out as part of Atatürk University Research Fund project (PN: 2009/89), and Scientific and Technical Research Council of Turkey (TUBITAK) (PN:107T822).

REFERENCES

Aydoğan Ş, Çinar K, Asil H, Coşkun C, Türüt A (2009). Electrical characterization of Au/ZnO Schottky contacts on n-Si. J. Alloy. Compd. 476:913-918.

Biber M, Temirci C, Turut A (2002). Barrier height enhancement in the Au/n-GaAs Schottky diodes with anodization process. J. Vac. Sci. Technol. B 20(1):10-13.

Buzás A, Geretovszy Z (2007). Patterning ZnO layers with frequency doubled and quadrupled Nd:YAG laser for PV application. Thin Solid Films 515:8495-8499.

Cembrero J, Busquets-Mataix D (2009). ZnO crystals obtained by electrodeposition:Statistical analysis of most important process variables. Thin Solid Films 517:2859-2864.

Dalchiele EA, Giorgi P, Marotti RE, Martin F, Barrado JRR, Ayouci R, Leinen D (2001). Electrodeposition of ZnO thin films on n-Si(100). Solar Energy Mater. Solar Cells 70:245-254.

Doggett B, Chakrabarti S, O'Haire R, Meaney A, McGlynn E, Henry MO, Mosnier JP (2007). Electrical characterisation of phosphorus-doped ZnO thin films grown by pulsed laser deposition. Superlattice. Microst. 42:74-78.

Erie JM, Li Y, Ivill M, Kim HS, Pearton SJ, Gila B, Norton DP, Ren F (2008). Properties of Zn3N2-doped ZnO thin films deposited by pulsed laser deposition. Appl. Surf. Sci. 254:5941-5945.

Fan JC, Xie Z, Wan Q, Wang YG (2007). As-doped p-type ZnO films prepared by cosputtering ZnO and Zn3As2 targets. J. Cryst. Growth 307:66-69.

Fang TH, Kang SH (2010). Preparation and characterization of Mg-doped ZnO nanorods. J. Alloy. Compd 492:536-542.

Fortunato E, Barquinha P, Pimentel A, Gonçalves A, Marques A, Pereira L, Martins R (2005). Recent advences in ZnO transparent thin film transistor. Thin Solid Films 487:205-211.

Güllü Ö, Biber M, Duman S, Türüt A (2007). Electrical characteristics of the hydrogen pre-annealed Au/n-GaAs Schottky barrier diodes as a function of temperature. Appl. Surf. Sci. 253:7246-7253.

Guo H, Zhou J, Lin Z (2008). ZnO nanorod light-emitting diodes fabricated by electrochemical approaches Electrochem. Commun. 10:146-150.

Inguanta R, Garlisi C, Spano T, Piazza S, Sunseri C (2013). Growth and photoelectrochemical behavior of electrodeposited ZnO thin films for solar cells. J. Electrochem 43:199-208.

Izaki M, Katayama J (2000). Characterization of boron incorporated zinc oxide film chemically prepared from an aqueous. J. Electrochem. Soc. 147:210-213.

Izaki M, Omi T (1997). Characterization of transparent zinc oxide films prepared by electrochemical reaction. J. Electrochem. Soc. 144:1949-1952.

Janotti A, Van de Wall CG (2009). Fundamentals of zinc oxide as a semiconductor Rep. Prog. Phys. 72:126501-1265029.

Jun W, Yintang Y (2008). Deposition of K-doped p type ZnO thin films on (0001) Al2O3 substrates. Mater. Lett. 62:1899-1901.

Kaminska E, Piotrowska A, Kossut J, Barcz A, Butkute R, Dobrowolski W, Dynowska E (2005). Transparent p-type ZnO films obtained by oxidation of sputter-deposited Zn3N2. Solid State Commun. 135:11-15.

Karataş Ş, Altindal Ş, Türüt A, Özmen A (2003). Temperature dependence of characteristic parameters of the H-terminated Sn/p-Si(100) Schottky contacts. Appl. Surf. Sci. 217:250-260.

Kim GH, Kim DL, Ahn BD, Lee SY, Kim HJ (2009). Investigation on doping behavior of copper in ZnO thin film. Microelectron. J. 40:272-275.

Kim IS, Jeong EK, Kim DY, Kumar M, Choi SY (2009). Investigation of p-type behavior in Ag-doped ZnO thin films by E-beam evaporation. Appl. Surf. Sci. 255:4011-4014.

Kim K, Lee K, Oh MS, Park CH, Im S (2009). Surface-induced time-dependent instability of ZnO based thin-film transistors. Thin Solid Films 517:6345-6348.

Kim KS, Kim HW, Kim NH (2003). Structral characterization of ZnO films grown on SiO2 by the RF magnetron sputtering. Physica B 334:343-346.

Krunks M, Dedova T, Karber E, Mikli V, Acik IO, Grossberg M, Mere A (2009). Growth and electrical properties of ZnO nanorod arroys prepared by chemical spray pyrolysis. Physica B 404:4422-4425.

Li Y, Xu L, Li X, Shen X, Wang A (2010). Effect of aging time of ZnO sol on the structural and optical properties of ZnO thin films prepared by sol-gel method. Appl. Surf. Sci. 256:4543-4547.

Lin SS, Lu JG, Ye ZZ, He HP, Gu XQ, Chen LX, Huang JY, Zhao BH (2008). p-type behavior in Na-doped ZnO films and ZnO homojunction light emitting diodes. Solid State Commun. 148:25-28.

Liu W, Gu SL, Ye JD, Zhu SM , Wu YX, Shan ZP, Zhang R, Zheng YD, Choy SF (2008). High temperature dehydrogenation for realization of nitrogen-doped p-type ZnO. J. Cryst. Growth 310:3448-3452.

McCluskey MD, Jokela SJ (2009). Defects in ZnO. J. Appl. Phys. 106:071101-0711013.

Mohanta SK, Kim DC, Cho HK, Chua SJ, Tripathy S (2008). Structral and optical properties of ZnO nanorods grown by metal organic chemical vapor deposition.s J. Cryst. Growth 310:3208-3213.

Mouet T, Devers T, Telia A, Mesai Z, Harel V, Konstantinov K, Kante I, Ta MT (2010). Growth and characterization of thin ZnO films deposited on glass substrates by electrodeposition technique. Appl. Surf. Sci. 256:4114-4120.

Pan X, Ye Z, Li J, Gu X, Zeng Y, He H, Zhu L, Che Y (2007). Fabrication of Sb-doped p-type ZnO thin films by pulsed laser deposition. Appl. Surf. Sci. 253:5067-5069.

Rhoderick EH, Williams RH (1998). Metal-Semiconductor Contacs, second ed., Clarendon Press, Oxford.

Sen Chien FS, Wang CR, Chan YL, Lin HL, Chen MH, Wu RJ (2010). Fast-response ozone sensor with ZnO nanorods grown by chemical vapor deposition. Sensor. Actuat. Phys. B 144:120-125.

Sharma SK, Rammohan A, Sharma A (2010). Templated one step electrodeposition of high aspect ratio n-type ZnO nanowire arrays. J. Colloid Interf. Sci. 344:1-9.

Song JH, Van Meirhaeghe RL, Laflére WH, Cordon F (1986). On the difference in apparent barrier heights as obtained from capacitance-voltage and current-voltage-temperature measurements on Al/p-InP Schottky barriers. Solid-State Electron. 29 633-638.

Soylu M, Yakuphanoglu F (2010). Analysis in of barrier height homogeneity in Au/n-GaAs Schottky barrier diodes by Tung model. J. Alloys Compd. 506:418-422.

Sullivan JP, Tung RT, Pinto MR, Graham WR (1991). Electron transport of inhomogeneous Schottky barriers:A numerical study. J. Appl. Phys. 70:7403-7424.

Tung RT (1992). Electron transport at metal-semiconductor interfaces: General theory. Phys. Review B 45:13509-13523.

Tüzemen S, Gür E (2007). Principal in issues producing new ultraviolet light emmiters based on transparent semiconductor zinc oxide. Opt. Mater. 30:292-310.

Wang C, Ji Z, Liu K, Xiang Y, Ye Z (2003). P-Type ZnO thin films prepared by oxidation of Zn3N2 thin films deposited by DC magnetron sputtering. J. Cryst. Growth 259:279-281.

Werner JH, Güttler HH (1991). Barrier inhomogeneities at Schottky contacts. J. Appl. Phys. 69:1522-1533.

Whangbo SW, Jang HB, Kim SG, Cho MH, Jeong KH, Whang CN (2000). Properties of ZnO thin films grown at room temperature by using ionized cluster beam deposition. Korean J. Phys. Soc 37(4):456-460.

Xiao B, Ye Z, Zhang Y, Zeng Y, Zhu L, Zhao B (2006). Facrication of p-type Li-doped ZnO films by pulsed laser deposition. Appl. Surf. Sci. 253:895-897.

Ye ZZ, Lu JG, Chen HH, Zhang YZ, Wang L, Zhao BH, Huang JY (2003). Preparation and characteristics of p-type ZnO films by DC reactive magnetron sputtering. J. Cryst. Growth 253:258-264.

Zhu BL, Zhao XZ, Su FH, Li GH, Wu XG, Wu J, Wu R(2010). Low temperature annealing effects on the structure and optical properties of ZnO films grown by pulsed laser deposition. Vacuum 84:1280-1286.

Zou CW, Chen RQ, Gao W (2009). The microstructures and electrical and optical properties of ZnO:N films prepared by thermal oxidation of Zn3N2 precursor. Solid State Commun. 149:2085-2089.